ELSEVIER

Journal of Nuclear Materials 313–316 (2003) 893–898

journal of nuclear materials

www.elsevier.com/locate/jnucmat

Numerical simulation of plasma profile changes in TEXTOR by externally driven radial polarization currents

H. Gerhauser [a,*,1], R. Zagórski [b], S. Jachmich [c,1], M. VanSchoor [c,1]

[a] *Institut für Plasmaphysik, Forschungszentrum Jülich GmbH, EURATOM Association, D-52425 Jülich, Germany*
[b] *Institute of Plasma Physics and Laser Microfusion, P.O. Box 49, 00-908 Warsaw, Poland*
[c] *Laboratoire de Physique des Plasmas, École Royale Militaire, EURATOM Association, Renaissancelaan 30, B-1000 Brussels, Belgium*

Abstract

An improved version of the 2D multifluid code TECXY is used to simulate polarization or biassing experiments on TEXTOR tokamak. In the numerical model the condition of globally ambipolar radial transport in the transition layer is replaced by externally driven radial polarization currents. They are produced by inserting and biassing an electrode with its tip a few centimeters inside the separatrix. The ensuing additional potential drop in the transition layer and the concomitant plasma profile changes are calculated for both signs of polarization. A comparison of modelling results with experimental measurements is presented. The fluid model reproduces some features of the L–H-like transition, but not the locally very high electric fields after bifurcation which are probably related to kinetic effects at very low collisionality.

PACS: 52.40.Hf; 52.55.Fa; 52.65.Kj
Keywords: Tokamak; Edge plasma modelling; Polarization experiment

1. Introduction

It was shown in experiments on TEXTOR tokamak [1,2] that large poloidal and toroidal flows and very high localized electric fields can be created in the edge plasma by electrode polarization or electrode biassing. (The words 'polarization' and 'biassing' are used synonymously throughout the paper, but 'polarization' is traditionally preferred by experimentalists for electrodes in the transition layer.) These flows vary rapidly in space and are believed to be responsible for the creation of transport barriers and improved confinement modes such as the H-mode. In an electrode biassing experiment, an electrode with its tip a few centimeters inside the separatrix forces a radial current through the plasma. This current is the main driving force of rotation and is balanced by friction mechanisms like viscosity as well as by interactions with neutrals.

In this paper we use an improved version of the 2D multifluid code TECXY [3–7] in order to analyze in more detail the changes to the plasma parameters in the edge of the TEXTOR tokamak induced by the applied polarization current. In order to describe the experimental situation the condition of globally ambipolar radial transport in the transition layer is replaced by externally driven radial polarization currents which are produced by inserting and biassing an electrode inside the separatrix. The ensuing additional potential drop in the transition layer and the concomitant plasma profile changes are calculated for both signs of polarization and different input parameters and compared with the experiment. Most interesting are the modifications to the global circulation layer (GCL) already existing in the

* Corresponding author. Tel.: +49-2461 61 5648; fax: +49-2461 61 2970.
E-mail address: h.gerhauser@fz-juelich.de (H. Gerhauser).
[1] Author affiliations are partners in the Trilateral Euregio Cluster (TEC).

0022-3115/03/$ - see front matter
PII: S0022-3115(02)01472-1

absence of polarization, where the poloidal plasma velocity goes all around the poloidal circumference. There is a complicated perpendicular force equilibrium between driving forces and counteracting forces (inertia, neutral friction, viscous forces), the driving forces being now enhanced and dominated by the Lorentz force from the imposed radial polarization current, which may further steepen the electric field and increase the shear of the rotational drift velocity, leading finally to a L–H transition.

2. Physical model

The 2D boundary layer code TECXY is primarily based on the classical transport equations derived by Braginskij [8] with the important additional assumption of anomalous cross-field transport. The model has been described elsewhere [3–7,9]. In the present paper we focus our consideration to the radial electric field and its dependence on the imposed electrode polarization. We use h_x, h_y, h_z as the metric coefficients ($\sqrt{g} = h_x h_y h_z$), and b_x, b_z are components of the unit vector parallel to the total magnetic field B. In order to determine the radial electric field $E_y \equiv (-1/h_y)\partial\Phi/\partial y$, which by the $E \times B$ electric drift mostly contributes to the poloidal flow, the plasma potential $\Phi(x, y)$ has to be found. In the model it is obtained by integrating Ohm's law ($\alpha_T = 0.71$) along magnetic field lines [9]:

$$\Phi(x,y) = \int_{x_o}^{x} \left(\frac{1}{en_e}\frac{\partial p_e}{\partial \xi} + \frac{\alpha_T}{e}\frac{\partial T_e}{\partial \xi} - \frac{h_x}{b_x}\frac{j_\parallel}{\sigma_\parallel} \right) \mathrm{d}\xi + \Phi_0(y), \tag{1}$$

where $\Phi_0(y)$ is determined by the boundary condition and $j_\parallel$ is the parallel plasma current, which in turn itself is a function of plasma potential. Thus the plasma current has to be also determined. The loop voltage $\oint(\partial\Phi/\partial\xi)\,\mathrm{d}\xi$ must always vanish.

It was shown in [5,9] that in the SOL, where the potential drop in the Langmuir sheath $\Delta\Phi$ is given by $\Delta\Phi = \Delta\Phi^{\mathrm{sh}} - (T_e/e)\ln(1 - j_x/\sum_a e_a n_a V_{ax})$ with $\Delta\Phi^{\mathrm{sh}}(\sim 3T_e/e)$ being the drop without poloidal current, the problem reduces to a strongly nonlinear equation which determines potential and currents in the SOL. In the transition layer, however, $\Delta\Phi = 0$ and the potential at one line (e.g. bisectrix, $x_0 = x_{\mathrm{bis}}$) has to be given in order to close the system of equations. It can be found from the global ambipolarity constraint [9] for a vanishing total current $J_y = \int\int j_y h_x \,\mathrm{d}x\, h_z \,\mathrm{d}z$:

$$\begin{aligned}\frac{J_y}{2\pi R_0} = &- \oint \frac{h_z h_x}{B}\left[\frac{b_z}{h_x}\left(2p + \sum_a (b_a + m_a n_a V_{a\parallel}^2) \right) \right.\\ &\left. \times \frac{\partial}{\partial x}\ln(h_z b_z) + \sum_a m_a c_s^a b_x P_2^a \right] \mathrm{d}x\\ &+ \oint \frac{h_z h_x}{B}\left[\sum_a m_a V_{a\perp}\left(P_1^a + S_n^a\right) \right.\\ &\left. + \sum_a m_a n_a \left(V_{ax}\frac{1}{h_x}\frac{\partial}{\partial x} + V_{ay}\frac{1}{h_y}\frac{\partial}{\partial y} \right) V_{a\perp} \right] \mathrm{d}x\\ &- \oint \frac{h_z h_x}{B}\frac{1}{\sqrt{g}}\frac{\partial}{\partial y}\left(\frac{\sqrt{g}}{h_y^2}\sum_a \eta_\perp^a \frac{\partial V_{a\perp}}{\partial y} \right) \mathrm{d}x = 0. \end{aligned} \tag{2}$$

Here R_0 is the major radius of the device, S_n^a is the particle source term and b_a is the parallel viscosity term. The source term from the momentum transfer with neutrals has been written as: $S_{V\perp}^a \equiv -m_a V_{a\perp} P_1^a + m_a c_s^a b_x P_2^a$, where c_s^a is the sound speed, and P_1^a, P_2^a are determined by atomic processes (rate coefficients for charge exchange, ionization and recombination) and the density distribution of neutrals as obtained from an analytical model. For deuterium with neutral density n_{D} we have $P_1^i = n_{\mathrm{D}}\alpha_{cx}^{\mathrm{D}} + n_i\beta_{\mathrm{rec}}^{\mathrm{D}}$, $c_s^i b_x P_2^i = n_{\mathrm{D}} v_{\mathrm{D}\perp}(\alpha_i^{\mathrm{D}} + \alpha_{cx}^{\mathrm{D}})$.

All other quantities have their usual meaning [7–9]. It has been shown [5,9] that the ambipolarity constraint (Eq. (2)) can be easily transformed into a linear differential equation of third order for the plasma potential at the bisectrix $\Phi^* \equiv \Phi(x_{\mathrm{bis}}, y)$:

$$B(y)\frac{\mathrm{d}\Phi^*}{\mathrm{d}y} + C(y)\frac{\mathrm{d}^2\Phi^*}{\mathrm{d}y^2} + D(y)\frac{\mathrm{d}^3\Phi^*}{\mathrm{d}y^3} = A_0(y) + A_1(y). \tag{3}$$

Here all coefficients are known functions of the plasma parameters. Especially $A_0(y)$ is given by the first integral of Eq. (2). We have split the right hand side of Eq. (3) into two parts, because only the coefficient $A_0(y)$ contains contributions from free forces acting on the plasma, whereas all terms in the coefficient $A_1(y)$ have corresponding parts on the left hand side of Eq. (3) (see [9]) and describe compensating or counteracting forces during the system evolution. The remaining free driving forces in $A_0(y)$ can be associated to the pressure force $(2p + \sum_\alpha b_\alpha)$, centrifugal force $(\sum_\alpha m_\alpha n_\alpha V_{\alpha\parallel}^2)$ and momentum input due to neutrals $(\sum_\alpha m_\alpha c_s^\alpha b_x P_2^\alpha$, N-term in Fig. 2).

2.1. Polarization of transition layer

The model presented above for the electric field is valid only in the case when the global ambipolarity condition is fulfilled which means that no external currents enter the integration domain. In order to model the polarization experiment it is necessary to assume additional radial currents crossing the core boundary. In the experiment an electrode is introduced to the plasma edge from the bottom of the TEXTOR vessel, and it is biassed with positive or negative voltage relative to the limiter and wall, which draws a polarization current I_{pol} through the plasma. In the model, however, we have to assume toroidal symmetry (for the current this has been

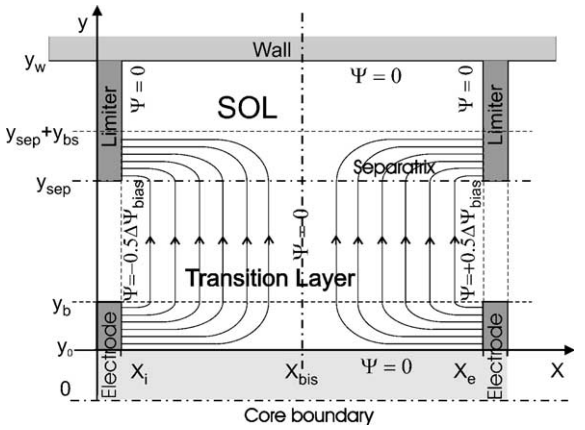

Fig. 1. Schematics of the additional polarization current from the electrode to the limiter (contour lines of the stream function Ψ).

proven experimentally), and we have to impose a suitable current distribution in our integration domain. For a positive bias voltage (Fig. 1) we have a positive current $J_{y\text{bias}}$ crossing the transition layer. It enters as a poloidal current from a radial interval at the position of the electrode, and it arrives again as a poloidal current at the limiter in a radial interval behind the limiter head. For simplicity we assume that the electrode is at the same poloidal position as the limiter, and that the imposed radial bias current is poloidally uniformly distributed. This does not mean that the resulting total radial current, which is self-consistently calculated and generated by the triggering bias current, must also be poloidally uniform. Quite on the contrary, it is strongly non-uniform, with local values being up to one order of magnitude larger than the uniform imposed current. Only the small bias current distribution is fully symmetric as depicted in Fig. 1, where the current is given by the contour lines of the following imposed stream function Ψ_{bias}:

$$\Psi_{\text{bias}}(x,y) = \Delta\Psi_{\text{bias}}\frac{x-x_{\text{bis}}}{x_e-x_i}f(y) = \frac{I_{\text{pol}}}{2\pi R_0}\frac{x-x_{\text{bis}}}{x_e-x_i}f(y) \quad (4)$$

with $0 \leqslant f(y) \leqslant 1$ being the specified profile function simulating the localized electrode current input and the current collection at the limiter (see e.g. s-shape of the J_y-term in Fig. 2). The stream lines give the polarization current density $\vec{j}_{\text{bias}}$ and are shown schematically in Fig. 1: $(\sqrt{g}/h_x)j_{x\text{bias}} = -(\partial\Psi_{\text{bias}}/\partial y), (\sqrt{g}/h_y)j_{y\text{bias}} = (\partial\Psi_{\text{bias}}/\partial x)$. The total radial polarization current is

$$J_{y\text{bias}}(y) = \oiint j_{y\text{bias}}h_x\,\mathrm{d}x h_z\,\mathrm{d}z = 2\pi R_0(\Psi_{\text{bias}}(x_e,y) - \Psi_{\text{bias}}(x_i,y)) = 2\pi R_0\Delta\Psi_{\text{bias}}f(y) \quad (5)$$

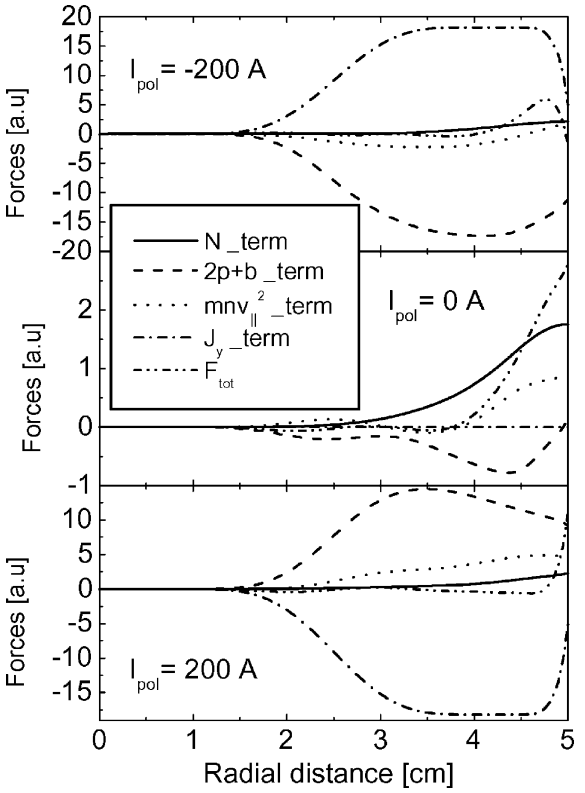

Fig. 2. Poloidally integrated driving forces for different polarization currents (neutrals, pressure gradients, centrifugal force and imposed Lorentz force).

or $I_{\text{pol}}f(y)$. This current replaces the zero current in our ambipolarity condition (Eq. (2)) and in the equation for the radial electric field (Eq. (3)). The function $A_0(y)$ in Eq. (3) is replaced by $A_0^{\dagger}(y) = A_0(y) - \Delta\Psi_{\text{bias}}f(y)$. Note that there is a freedom in the model how the polarization current should be distributed between ions and electrons. We assumed that the current is carried either by ions or equally divided between ions and electrons, but the influence of this partition on the results of calculations is rather weak.

3. Results of calculations and discussion

We used standard boundary conditions in our calculations [7]. The computational domain extends poloidally from one limiter side to the other limiter side and radially from $r = 41$ cm ($y = 0$ cm) to $r = 50$ cm ($y_w = 9$ cm) with the separatrix at $a = 46$ cm ($y_{\text{sep}} = 5$ cm). At the core boundary total power and particle input fluxes are specified. At the wall we have prescribed decay lengths, and at the limiter standard sheath conditions are specified. In order to analyze the influence of different physical mechanisms and of the polarization current I_{pol} on

plasma parameters and electric field, we have performed calculations with the TECXY code for TEXTOR tokamak discharges in deuterium but neglected the effect of impurities (the influence of impurities on the electric field structure is not decisive [6]). The belt limiter ALT-II is at $\theta = -45°$ position, the total magnetic field $B = 2.33$ T, the plasma current $I_p = 210$ kA and the Shafranov shift $\Delta = 6$ cm. The magnetic flux surfaces are shifted circles as calculated from the analytical model in [9]. We use the anomalous radial transport coefficients $\eta_y = (1/3)m_i n_i D_y$ and $\chi_y^e/n_e = (3/2)(\chi_y^i/n_i) = 2D_y$ with $D_y = 1.5$ m^2/s (including an Alcator-like decrease with density towards the core). The standard value for the input particle flux to the SOL is $\Gamma_{inp} = 2.5 \times 10^{21}$ s^{-1} and for the power input $Q_{inp} = 0.4$ MW with the recycling coefficient equal to $R = 0.7$, meaning that 70% of the recycled neutrals were reionized in the boundary layer.

It was shown in [6] that the electric field and the plasma flow in the transition layer are mainly determined by the interplay between the different forces in the $A_0(y)$ coefficient. In Fig. 2 we have plotted the poloidally integrated forces occurring in $A_0^{\dagger}(y)$ for zero and two extreme polarization currents I_{pol}. Without radial current the total force is positive and mainly determined by the centrifugal force as well as by the non-compensated (by pressure action) part of the momentum input from neutrals. This yields the usual counterclockwise global circulation of the plasma inside the separatrix in a layer (GCL) of about 1 cm width. Adding a polarization current I_{pol} strongly influences the force balance. Most interestingly the effect of I_{pol} is largely compensated by the plasma reaction (pressure term), and consequently strong poloidal gradients of plasma parameters develop in the transition layer. These gradients produce locally very large radial currents which exceed by more than one order of magnitude the average input radial current. The negative polarization currents enhance the naturally appearing GCL, whereas the positive currents tend to reverse the plasma flow to clockwise direction. Corresponding changes to radial plasma profiles are shown in Figs. 4 and 5. It can be seen that the plasma potential Φ in the transition layer is strongly affected by the polarization currents. The changes in Φ are reflected in the radial electric field E_y, which via the $E \times B$ drift modifies significantly the plasma flows in the boundary layer. The reversal of I_{pol} also reverses the negative peaks of E_y and poloidal velocity V_x to positive.

In Fig. 3 the calculated I–V characteristics is shown together with experimental points. The modelling points correspond to the above mentioned series of calculations with standard input parameters as well as to cases with lower input particle and energy fluxes ('*low density*': $\Gamma_{inp} = 1.3 \times 10^{21}$ s^{-1}, $Q_{inp} = 0.3$ MW; '*very low density*': $\Gamma_{inp} = 0.8 \times 10^{21}$ s^{-1}, $Q_{inp} = 0.09$ MW with three times enhanced heat conductivities in order to be more consistent with the very flat experimental temperature profiles observed before and after the bifurcation, but there remains a discrepancy between experiment and modelling). In the 'scan' the diffusion coefficient D_y has been reduced from 1.5 m^2/s ($I_{pol} = 0$ A) to 0.7 m^2/s ($I_{pol} = 200$ A) while keeping the input fluxes at the standard values. This allowed to be more consistent with the experimental steepening of density profiles close to the bifurcation. Then the input fluxes were reduced together from standard values to $\Gamma_{inp} = 0.9 \times 10^{21}$ s^{-1} and $Q_{inp} = 0.12$ MW ($I_{pol} = 60$ A) while keeping $D_y = 0.7$ m^2/s constant. Note that the I–V characteristics for negative biassing is hypothetical, because the ion saturation current of the small electrode would limit the negative I_{pol} to very small values. In the I–V characteristics as obtained from simulations we can distinguish two branches: a growing branch where the polarization current increases almost linearly with the applied voltage, and a decaying branch where I_{pol} decreases together with the input fluxes, but the polarization potential remains high. In experiment the growing branch of the I–V characteristics is associated with L-mode discharges, whereas the decaying branch (two data points) corresponds to a transition to H-mode-like behaviour. Obviously some kind of bifurcation develops. Since a bifurcation to H-mode in principle means reduction of transport, both of particles and energy, such a behaviour is appropriately simulated in calculations by reduction of input particle and energy fluxes keeping simultaneously I_{pol} as high as possible. The limit in I_{pol} simply reflects the limit of the saturation current which can be collected by the limiter, and this limit is in turn determined by and reduced along with the provided input particle fluxes.

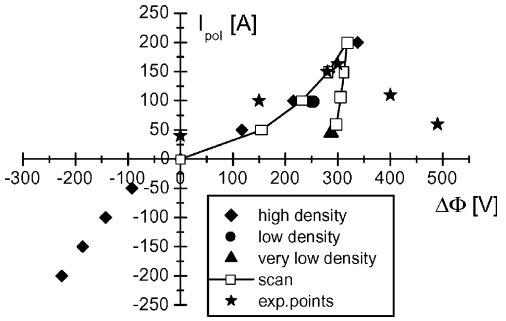

Fig. 3. Measured (experimental points) and calculated (for different modelling assumptions) I–V characteristics for TEXTOR.

In Fig. 4 we have plotted the radial profiles of electric field and plasma velocities also for an experimental L-mode discharge with $I_{pol} = 163$ A. Very remarkably there is almost quantitative agreement with the modelling results for 200 and 100 A (*low density case*). In the fast rotating layer inside the separatrix, the electric drift velocity E_y/B amounts to about 80% of the poloidal velocity V_x. After transition to 'H-mode' the experimental

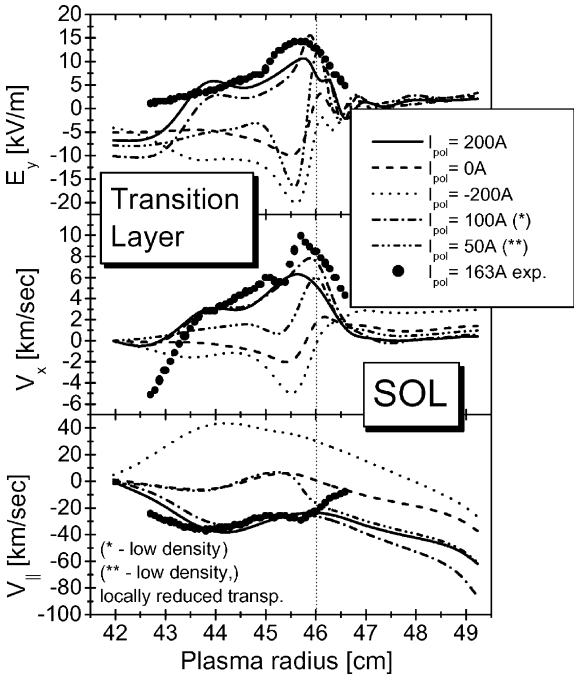

Fig. 4. Radial profiles of electric field and velocities V_x, $V_\parallel$ at LFS. Comparison of different modelling results with experimental L-mode just before bifurcation.

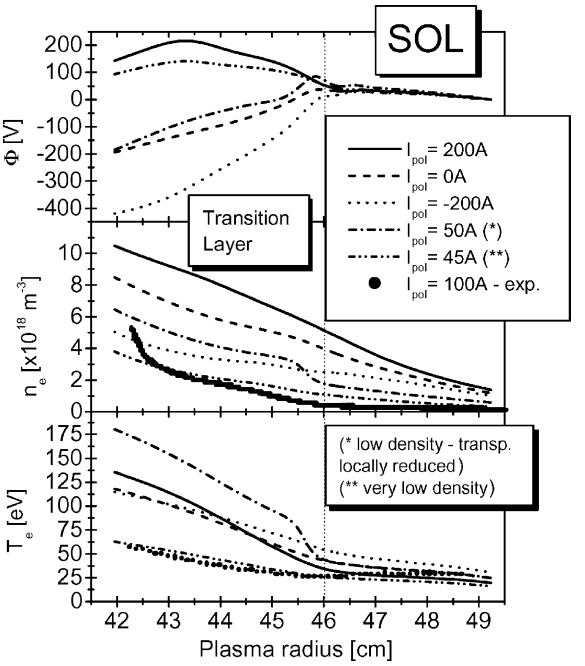

Fig. 5. Radial profiles of plasma potential, density and temperature at LFS for different modelling assumptions. Included are also typical experimental L-mode n_e and T_e profiles.

E_y and V_x values are about three times larger in a 1 cm wide interval inside the separatrix, but almost unchanged elsewhere. This is reflected in the I–V characteristics (Fig. 3) by the very right experimental point with 490 V polarization voltage. It is impossible to simulate such conditions by the code because of the model limitations (fluid approximation). For very low plasma density and collisionality there is a transition to detachment and to plateau and banana regime in a typically 1 cm wide interval inside the separatrix. This suggests the conjecture that the large electric fields in this interval may be related to kinetic effects like orbit squeezing [1,2] and cannot be described by our fluid theory. However, some tendencies are even reflected by our numerical solution: for lower plasma density the bifurcated solution is achieved with smaller polarization current and simultaneously locally higher radial electric field.

We have also plotted some typical experimental L-mode density and temperature profiles in Fig. 5. The puzzling fact is that with increasing $I_{\rm pol}$ the experimental density profiles (which could not all be included in this paper) become steeper and steeper (everywhere in the transition layer, not only locally), but the T_e profiles (also not shown) on the contrary become flatter and flatter, even horizontal after bifurcation. Hence on the one hand it appears that anomalous diffusion tends to be reduced, but on the other hand the anomalous heat conductivity is drastically increased. This can be simulated artificially like in our *very low density case* (see Fig. 5), but this does not correspond to the typical behaviour of a spontaneous L–H transition, where diffusivity and heat conductivities are both reduced. Furthermore we would expect only a local transport barrier with pedestal-like profiles, which are connected with a negative electric field spike, see e.g. results in DIII-D [10]. Indeed, we have inserted in Figs. 4 and 5 also the profiles for a 'low density case' with locally (close to $r = 45.5$ cm) 10 times reduced transport coefficients, and we see a negative electric field spike of about −15 kV/m (almost quantitatively like in [10]) connected with locally very steep and pedestal-like profiles of n_e and T_e. Hence we can reproduce the signatures of true L–H transitions, but the polarization-induced quasi-L–H transition in the TEXTOR experiments shows different signatures related rather to detachment at very low density and collisionality.

4. Conclusions

In the present paper we use the TECXY code to simulate polarization experiments in TEXTOR tokamak. The polarization current has been introduced to the model by imposing an additional stream function. Calculations have been performed for both signs of the polarization current, and the plasma profiles have been compared to experiment. It appears that the plasma potential and plasma flows in the edge region are strongly

affected by the polarization currents. The code results are able to reproduce, sometimes almost quantitatively, experimentally observed radial profiles of plasma parameters as well as the I–V characteristics. The agreement is especially good for L-mode discharges, whereas for the bifurcation to H-mode only tendencies can be reproduced. The discrepancy at very low plasma density may be connected to the limitations of the fluid model as well as to the fact that the observed polarization-induced L–H transitions in TEXTOR experiments seem to be related rather to plasma detachment and to transport changes by kinetic effects at very low collisionality.

Acknowledgement

This work was supported in part by Grant (No. 2 P03B 057 22) from the Polish Committee for Scientific Research.

References

[1] M. VanSchoor, S. Jachmich, An experimental and theoretical study of suppression of ..., paper P3-70, these proceedings.
[2] M. VanSchoor, H. VanGoubergen, R.R. Weynants, J. Nucl. Mater. 290–293 (2001) 962.
[3] R. Zagórski, H. Gerhauser, H.A. Claaßen, J. Nucl. Mater. 266–269 (1999) 1261.
[4] R. Zagórski, H. Gerhauser, H.A. Claaßen, J. Techn. Phys. 40 (1) (1999) 99.
[5] H. Gerhauser, R. Zagórski, et al., J. Nucl. Mater. 290–293 (2001) 609.
[6] R. Zagórski, H. Gerhauser, et al., Contrib. Plasma Phys. 42 (2–4) (2002) 247.
[7] H. Gerhauser et al., Nucl. Fusion 42 (2002) 805.
[8] S.I. Braginskij, Rev. Plasma Phys. 1 (1965) 205.
[9] R. Zagórski et al., Report of FZ Jülich, JÜL-3829, November 2000.
[10] P. Gohil et al., Nucl. Fusion 34 (8) (1994) 1057.